MODE II DELAMINATION OF CFRP-METAL LAMINATES AT BOLTED JOINTS

J. Both*, D. Barfuß, H. Baier
TU München, Institute of Lightweight Structures, Munich, Germany
*Corresponding author (both@llb.mw.tum.de)

Keywords: *mode II delamination, fiber metal laminate, bearing strength*

1 Introduction

In order to improve the bearing strength of carbon fiber reinforced plastics (CFRP) at bolted joints thin metal sheets are laminated into the load application area of reinforced plastics. The bearing strength is increased significantly through alternating stacking of unidirectional (UD) CFRP layers and titanium or steel layers [1-3]. One disadvantage of this procedure is that stress concentrations build up at the butt joints between metal and CFRP layers as a result of changes in stiffness and differences in the thermal expansion behavior (schematic illustration see Fig. 1.).

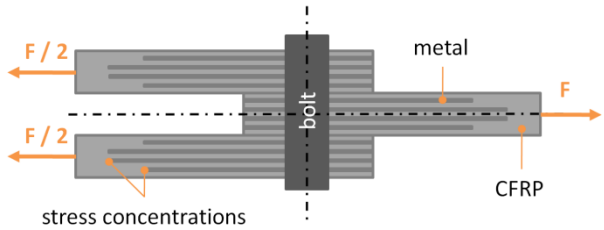

Fig. 1: Schematically: hybrid CFRP-metal bolted joint

The stress concentrations initiate matrix fracture in the neighboring +45°, -45° and 90° layers and define starting points for mode II delaminations when applying tension load to the laminate. This paper contributes to the understanding of the failure mechanisms of these fiber metal laminates (FML) at bolted joints.

2 Experimental determination of the critical energy release rate G_{IIc}

2.1 Delamination modes

Three main delamination modes, mode I, II and III (see Fig. 2) occur in fiber reinforced plastics according to the loading direction. Mode II describes the fracture mode in which the delamination faces slide over each other in the direction of the delamination growth [4]. This is the most likely mode to occur after matrix failure at the butt joints between CFRP and metal layers in hybrid metal-CFRP laminates at symmetrically loaded bolted joints.

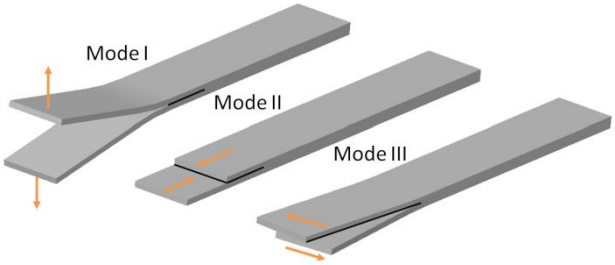

Fig. 2: Delamination modes of fiber reinforced plastics

Currently standardized testing methods for polymer matrix composites only exist for mode I and mixed mode I – mode II delaminations [4, 5]. To the author's knowledge standard test methods for FML do not exist for neither of the above mentioned modes. Since the beginning of 2009 a work item (WK22949) was initiated by the American Society for Testing and Materials (ASTM) with the scope to standardize a test method for mode II delaminations for UD fiber reinforced composites [6]. The tests are carried out on End Notched Flexure (ENF) specimens which therefore are applied in this study as well.

2.2 End Notched Flexure test

In order to preserve the critical energy release rate G_{IIc}, which is a necessary input parameter for the performed Finite Element (FE) simulations, ENF tests were carried out on hybrid CFRP-steel (st) laminates using a three point bending test. The materials used are UD prepregs (specification: Sigrafil

CE 1250-230-39) and 0.25 mm thin steel sheets (specification: AISI 301). The cured prepregs also exhibit a thickness of approximately 0.25 mm. Herewith a substitution of CFRP layers in a hybrid laminate will not lead to thickness variations. Two stack-ups ($[0/st/0/st/0/st]_2$ and $[90/st/90/st/90/st]_2$) were investigated. The notch at one end of the specimens was realized by laminating a 50 µm thin Teflon foil into the layup after the 6th lamina. This splits the specimen into two beams with identical layups. During the test the initial notch propagates to the middle of the specimen where the load is applied. A photograph of the test setup is shown in Fig. 3.

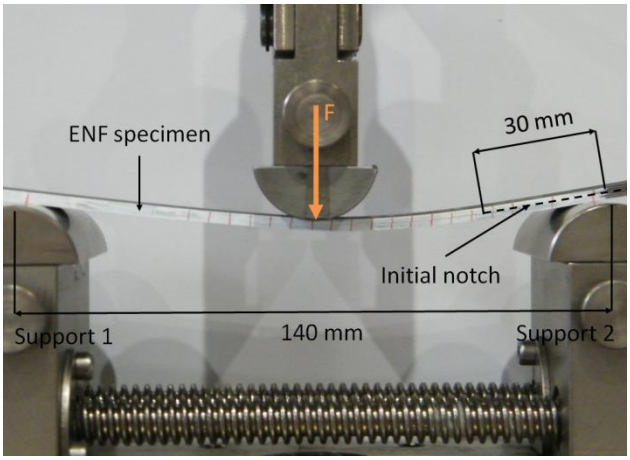

Fig. 3: Setup ENF test

According to [7] G_{IIc} may be determined by direct application of the beam theory (BT), which is applicable in this case as the two beams of the split specimen have the same layup:

$$G_{IIc}(BT) = \frac{9a^2 P\delta}{2b(2L^3 + 3a^3)} \qquad (1)$$

In formula (1) a is the crack length, δ the deflection when the maximum force P is applied during the bending test, b the specimen width and $2L$ the specimen length. To account for geometric nonlinearities as well as for the displacement of the load application point with reference to the delamination axis the following correction factors k, F and N (see formulas 2, 3 and 4) are introduced as proposed in [7], where E_b is the bending modulus of the split beams and G_{13} the corresponding shear modulus. The latter may be determined by the classical lamination theory (CLT).

$$k = 1 + 0{,}2\,\frac{E_b h^2}{G_{13} a^2} \qquad (2)$$

$$F = 1 - 0{,}6099\left(\frac{\delta}{L}\right)^2 \qquad (3)$$

$$N = 1 + 0{,}3766\left(\frac{\delta}{L}\right)^2 \qquad (4)$$

The factors lead to a corrected version of the BT, the "corrected beam theory" (CBT), which is stated in formula (5):

$$G_{IIc}(CBT) = G_{IIc}(BT)k\,\frac{F}{N} \qquad (5)$$

The mean values of the critical energy release rates gained from the test results and calculated via the CBT and their standard deviation σ are listed in Table 1. 6 specimens of each configuration were tested.

	$[0/st/0/st/0/st]_2$	$[90/st/90/st/90/st]_2$
G_{IIc} (CBT)	820 N/m	809 N/m
σ	207 N/m	102 N/m

Table 1: critical energy release rates G_{IIc} (CBT) and standard deviations σ for 0° and 90° specimens

3 Simulation

3.1. Material characterization and modeling

The utilized CFRP shows an orthotropic, almost linear-elastic behavior until failure. In fiber direction it is slightly increasing, perpendicular to it decreasing especially at higher strain levels. As the thin steel sheets are produced through a cold rolling process which deforms the material strongly into the rolling direction, the sheets show orthotropic behavior. Differences in Young's moduli and strains to failure in both directions of approximately 15 % exist. A comparison of typical stress-strain graphs of the steel in both rolling (0°) and normal to rolling direction (90°) and the CFRP in fiber direction (0°) is shown in Fig. 4.

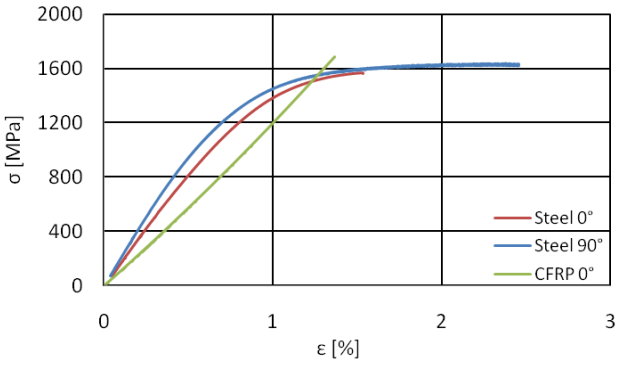

Fig. 4: σ-ε graphs of steel (0° and 90°) and CFRP (0°)

The coefficients of thermal expansion (CTE) of UD fiber reinforced plastics in 0° and 90° direction differ approximately by a factor of 100 while the deformations caused by temperature differences of the steel is almost equal in 0° and 90° direction (see Fig. 5). Please note that in Fig. 5 two graphs are plotted which show very similar progressions.

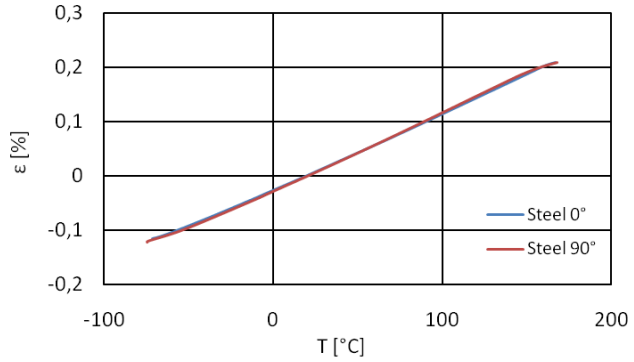

Fig. 5: Thermal strain of steel (0° and 90°)

The above mentioned material characterization provides the basis for the material models which are implemented in ABAQUS/Standard. For both CFRP and steel an orthotropic material law showing the following values was chosen (see Table 2).

	CFRP	steel
E_1 [MPa]	123.000	175.000
E_2 [MPa]	8.000	199.000
G_{12} [MPa]	4.500	72.000
ν_{12} [-]	0,30	0,32

Table 2: orthotropic material properies of CFRP and steel

The CTEs of CFRP and steel are listed in Table 3:

	CFRP	steel
α_1 [10^{-6}/K]	0,3	14,0
α_2 [10^{-6}/K]	30,0	14,0

Table 3: CTEs of CFRP and steel

The anisotropic yielding was also accounted for using ABAQUS' description of the Hill yield surface. Therefore the yield stress – yield strain progression is linearly interpolated through six interplation points (see Table 4).

Yield stress [MPa]	Yield strain [‰]
695	0,00
1.000	0,35
1.250	0,97
1.430	1,92
1.540	3,29
1.610	5,89

Table 4: interpolation parameters for the description of the yielding of the steel layers

In order to consider the anisotropy of yielding yield ratios (R_{ij}) have to be specified (see table 5). For the calculation of these values the parameters r_0, r_{90} and r_{45} were determined through tensile tests of the steel specimens. The specimens were cut at an angle of 0°, 90° and 45° with respect to the rolling direction.

	Yield ratio [-]	Yield ratio [-]
R_{11}	1	1,000
R_{22}	$\sqrt{\frac{(r_{90}(r_0+1)}{(r_0(r_{90}+1)}}$	1,135
R_{33}	$\sqrt{\frac{(r_{90}(r_0+1)}{r_0+r_{90}}}$	1,004
R_{12}	$\sqrt{\frac{3(r_0+1)r_{90}}{(2r_{45}+1)(r_0+r_{90})}}$	1,085
R_{13}	1	1,000
R_{23}	1	1,000

Table 5: Yield ratios for steel

3.2. Virtual Crack Closure Technique (VCCT)

The VCCT was used to simulate the ENF test and therewith verify the accuracy of G_{IIc}. The technique is implemented in ABAQUS/Standard and assumes that the same energy which is necessary to close an existing crack is responsible for its opening.
As the unsymmetric layup leads to warping of the specimens at room temperature the deflection of the specimen under a thermal load of ΔT = -100 °C was also accounted for. Good correlation between FEM and experiment was found so that the VCCT may be used for the delamination simulations at bolted joints.

3.3 Delamination at bolted joints

A FE-Model of a specimen to determine its bearing strength was designed according to DIN EN 6037 (see Fig. 6.). The basic laminate only consists of CFRP while the Transition zone and the Hybrid bolted joint consist of steel and CFRP layers (also compare to Fig. 1.).

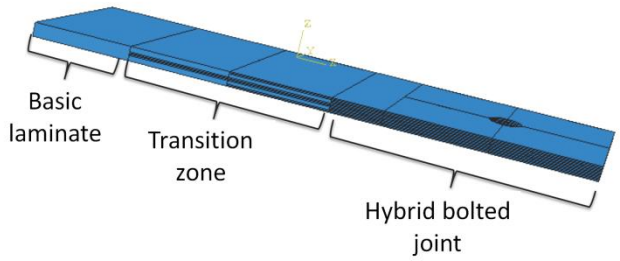

Fig. 6: FE-model of bearing strength specimen

The application of these hybrid laminates in load application areas is especially interesting for aerospace structures with one preferential load direction. Therefore CFRP laminates with a fraction of 70 % UD 0° layers, 15 % 90° layers and 15 % ±45° layers [70/15/15] are investigated subsequently. First the 90° layers of the basic laminate are substituted by the thin steel sheets then the ones laminated at ±45° with respect to the load direction. At last, to reach a maximum metal content in the bearing area, 0° lamina are replaced by steel. The investigated layup is schematically displayed in Figure 7.

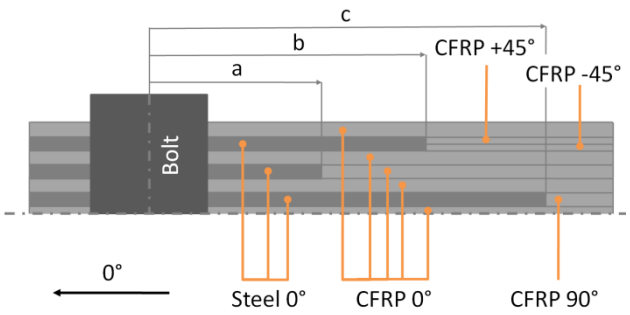

Fig. 7: investigated laminate configuration

The parameters *a*, *b* and *c* in Figure 7 were varied in order to investigate their influence on the onset of mode II delaminations during bearing loading the hybrid laminate. As the application of the VCCT requires a possible starting point for delaminations, the butt joints between the ± 45° CFRP and the steel layers as well as the ones between the 90° CFRP and the steel layers were not numerically connected. Due to high differences in the elastic behavior at these joints a transverse crack which may result in a delamination is most likely to occur here. Furthermore the failure criterion by Hashin was implemented to estimate the CFRP's laminate effort during bearing loading.

4 Results and conclusions

It was found that for the considered material combination and layup the bearing strength (here 2160 MPa, defined by a widening of the borehole by 2 % of the hole diameter) is reached before the onset of mode II delamiations for each laminate configuration investigated. The configurations are listed in table 5 (also see Fig. 7).

Configuration No..	a [mm]	b [mm]	c [mm]
1	20	40	60
2	30	50	70
4	50	70	90
6	70	90	110

Table 5: tested laminate configurations (also see Fig. 7)

In the 1st configuration (c = 60 mm) the maximum load that maybe transferred before the onset of delamination is slightly lower than at the other configurations. Consequently a minimum of c = 70 mm should be maintained in order to exploit the maxi-

mum load transfer before delamination onset (see Fig. 8).

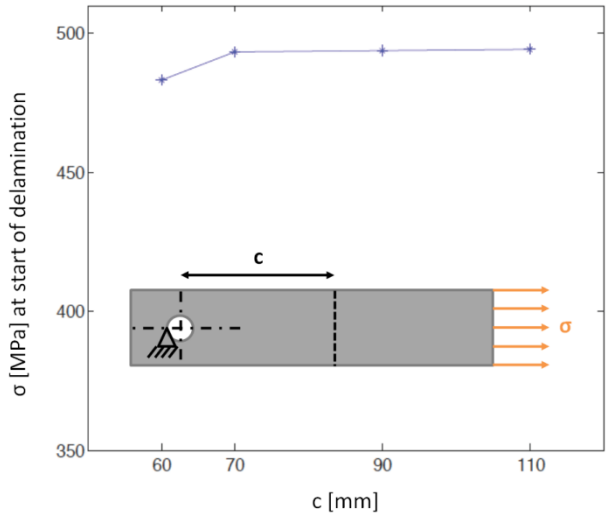

Fig. 8: Stress at start of delamination over steel length

The mode II delaminations always start at the butt joints between the CFRP 90° layer and the thin steel sheets considering the parameters of Table 5, see Fig. 9.

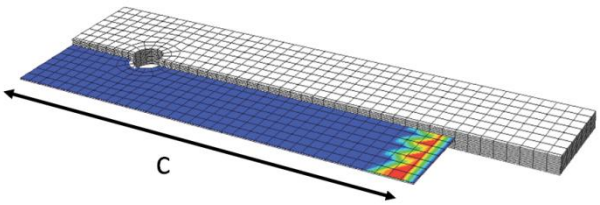

Fig. 9: Mode II energy release rate at butt joint between CFRP 90° and steel layer (also see Fig. 7)

This paper shows that mode II delaminations at bolted joints of hybrid CFRP-steel laminates are unlikely to occur before the borehole is opened by 2% and therefore may be classified as unproblematic at the investigated laminate – loading configurations. Further work includes the experimental validation of the stated conclusions as well as considering other laminate and material configurations.

Acknowledgement

This work originates from the project "HyCoS – Hybrid Composite Structures" which is headed by RUAG Aerospace and financed by the German Federal Ministry for Education and Research (Bundesministerium für Bildung und Forschung – BMBF) in cooperation with the German Aerospace Center (DLR).

References

[1] P.P. Camanho, A. Fink, A. Obst, S. Pimenta "Hybrid titanium-CFRP laminates for high-performance bolted joints. *Composites Part A*, Vol. 40, pp. 1826 – 1837, 2009

[2] A. Fink, P. Camanho, M. Canay, A. Obst "Increase of bolted joint performance by means of lokal laminate hybridization". *Processdings of the 1st CEAS European Air and Space Conference*. Berlin, Germany, pp 939 – 948, 2007

[3] J. M. Hudley, J.-M. Yang, H. T. Hahn "Bearing strength analysis o hybrid titanium composite laminates". *AIAA Journal*, Vol. 46, pp. 2074 – 2085, 2008

[4] ASTM D 6671 – 01: "Test method for mixed mode I-mode II interlaminar fracture toughness of unidirectional fiber reinforced polymer matrix composites"

[5] ASTM D 5528: "Test method for mode I interlaminar fracture toughness of unidirectional fiber-reinforced polymer matrix composites"

[6] ASTM WK22949: "New test method for determination of the mode II interlaminar fracture toughness of unidirectional fiber reinforced polymer matrix composites using the End-Notched Flexure (ENF) test"

[7] A. B. de Morais "Analysis of mode II interlaminar fracture of multidirectional laminates". *Composites Part A*, Vol 35, pp 51-57, 2004